

**Research  
Report****Synthesis of Mono-dispersed Spherical Mesoporous Silica**

Kazuhisa Yano

**Abstract**

Mono-dispersed spherical mesoporous silica was synthesized from tetramethoxysilane and alkyltrimethylammonium bromide ( $C_n$ TMABr) with short alkyl-chain as a surfactant under very specific conditions. Regularity of mesopores was high when dodecyltrimethylammonium ( $C_{12}$ TMABr) was used. The particle size was found controllable by changing synthesis

temperature, water/methanol ratio, and silica source while mono-dispersion characteristics were retained when decyltrimethylammonium bromide ( $C_{10}$ TMABr) was used. The obtained mono-dispersed spherical mesoporous silica had a particle size equivalent to the wave length of visible light, and thus its application to an optical use such as photonic crystal is expected.

**Keywords**

Mono-dispersed, Hexagonal, Mesoporous, Particle size, Sphere, Silica

## 1. Introduction

It has become possible to synthesize mesoporous silica having ordered pores by surfactant-templated method.<sup>1, 2)</sup> Pore diameter is controllable by varying the alkyl-chain length of the surfactant. Various studies are being conducted concerning application of mesoporous silica to catalysts, adsorbents, separation columns, and the like, by utilizing its uniform pore diameter characteristic. Morphology control is one of the major challenges for industrial use of mesoporous silica, and recent studies has focused on synthesizing particles with various shapes such as fiber-like,<sup>3-5)</sup> film-like,<sup>6)</sup> polyhedral,<sup>7-9)</sup> and spherical.<sup>10-12)</sup> Spherical particles are very promising for the use in chromatography, cosmetics or the like. For these purposes, synthesis of spherical particles with uniform particle size is essential.

Stöber et al. found that mono-dispersed silica particles can be synthesized from water, alcohol, ammonia, and tetraalkoxysilane.<sup>13)</sup> There have been attempts to synthesize mono-dispersed spherical mesoporous silica by a modified Stöber method involving further adding a template of such as alkyl amines.<sup>14-17)</sup> So far, only a few reports exist concerning the synthesis of mesoporous silica spheres with both a uniform morphology and an ordered mesoporous regularity.

Several methods have been reported for the synthesis of mesoporous materials. A hydrothermal synthesis in a high-pressure bottle is widely adapted, where precise control of the precipitation is rather difficult. In other cases, for example FSM<sup>18)</sup> where material is synthesized by gradual precipitation upon the continuous addition of a dilute HCl solution, the resulting composition of FSM material is far from uniform, because precipitation occurs at different times and pH. In similar synthesis processes, surfactant-templated silica (STS) could be obtained from C<sub>16</sub>TMABr and tetramethoxysilane (TMOS) in a water-alcohol mixture at ambient temperature.<sup>19, 20)</sup> During the synthesis, a clear transparent solution gradually becomes turbid, and then precipitation occurs. This has made STS to be a potential method with controlled precipitation toward the formation of uniform mesoporous silica materials.

Here, we describe the synthesis of spherical

mesoporous silica with both a uniform morphology and an ordered mesoporous regularity. We also describe a method for controlling the particle size of mono-dispersed spherical mesoporous silica. The materials were characterized using X-ray diffraction, TEM and SEM.

## 2. Experimental section

### 2.1 Synthesis

C<sub>10</sub>TMABr, C<sub>12</sub>TMABr, C<sub>16</sub>TMABr, TMOS (Tokyo Kasei), 1 M sodium hydroxide solution and methanol (Wako Inc.) were used without further purification. In a typical synthesis, 1.54 g of C<sub>10</sub>TMABr and 2.28 g of 1 M sodium hydroxide solution were dissolved in 397.7 g of water/methanol (75/25=w/w) solution. Then 1.32 g of TMOS was added to the solution with vigorous stirring. After the addition of TMOS, the clear solution gradually turned opaque due to the formation of a white precipitate. After 8 h of continuous stirring, the mixture was aged overnight. The white powder was then filtered and washed with distilled water at least three times, and then dried at 318 K for 72 h. The powder obtained was calcined in air at 823 K for 6 h to remove organic species.

### 2.2 Characterization

The calcined samples were stored under nitrogen atmosphere to prevent water adsorption, with which the peak intensity of X-ray diffraction would be largely abolished and the gas adsorption capacity would be decreased. X-ray diffraction measurements were carried out with a Rigaku Rint-2200 X-ray diffractometer using Cu-K $\alpha$  radiation. Since the shapes of samples synthesized were spherical, particles were equally placed in an X-ray holder without any orientation; this alignment led to a reproducible result (intensity). Argon adsorption isotherm was obtained with a Quantachrome Autosorb-1 at 87 K; samples were evacuated at 353 K under 10<sup>-3</sup> mmHg before measurement. Transmission electron micrograph was obtained with a Jeol-200CX TEM using an acceleration voltage of 200 kV. Scanning electron micrographs (SEM) were obtained with a SIGMA-V (Akashi Seisakusho); the surfaces of samples were coated with gold.

### 3. Results and discussion

#### 3.1 Synthesis of mono-dispersed spherical mesoporous silica with ordered hexagonal regularity

$C_{16}$ TMABr is the mostly used template for the synthesis of mesoporous silica. Usually, the regularity of the mesopores of materials obtained from  $C_{16}$ TMABr was very high. Therefore, on the basis of STS synthesis, reactants ( $C_{16}$ TMABr and TMOS) concentration was changed in order to obtain a mono-dispersed spherical mesoporous silica. The summarized results for the shapes and the uniformities of the particles are shown in **Table 1**, and the TEM photographs of the particles are shown in **Fig. 1**. The shapes of the particles obtained were irregular when the concentration was higher (H1, H5, H8). Although spherical particles were formed only in lower concentration conditions (H11, H13), mono-dispersed particles were not obtained. Longer precipitation time of H11 and H13 indicates that when the reaction proceeds slowly, shapes of particles become spherical. Generally, the formation of spherical particles is preferable when surface energy of a particle would be minimized. Therefore, it is important for obtaining spherical particles to have reaction proceed slowly. Mesoporous silica consists of both an inorganic silica part and an organic surfactant part. Hydrophobic interaction of a surfactant in a hydrophilic solution as well as condensation of silica precursors leads to a precipitation of mesoporous materials from a solution. On the basis of this aspect, shorter alkyl-chain surfactants with weaker hydrophobic interaction were used as a surfactant in order to obtain a spherical particle. Then,  $C_{12}$ TMABr was used as a surfactant. The summarized results for the shapes and the uniformities of the particles

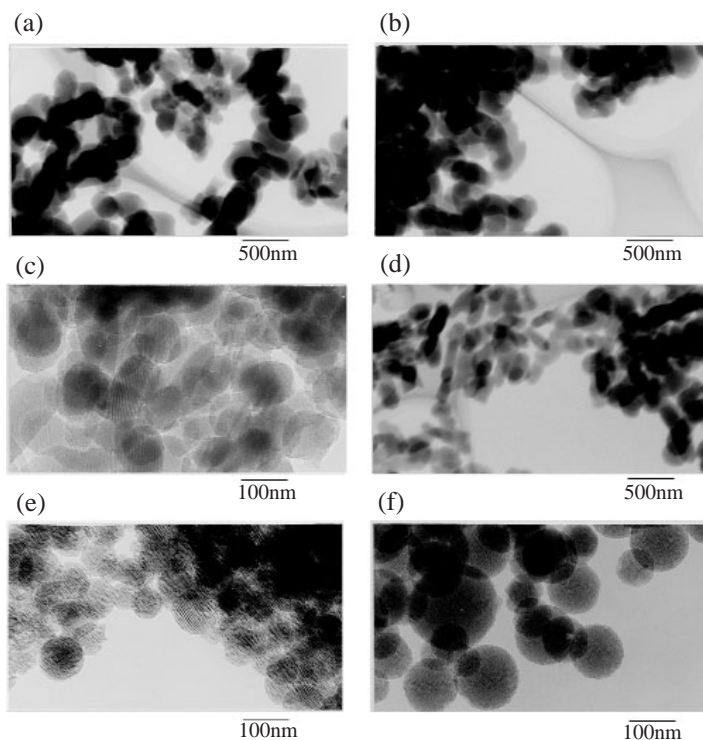


**Fig. 1** Transmission electron micrographs of (a) H1, (b) H5, (c) H8, (d) H10, (e) H11, and (f) H13.<sup>21)</sup>

**Table 1** Shapes of particles obtained from  $C_{16}$ TMABr and TMOS.<sup>21)</sup>

No.	Concentration of $C_{16}$ TMABr [mol/l]	Concentration of TMOS [mol/l]	$C_{16}$ TMABr/ TMOS*	Precipitation time** [sec]	Shapes of particle
H1	0.052	0.41	0.13	6	irregular
H2	0.052	0.20	0.26	_***	_****
H3	0.052	0.14	0.37	_***	_****
H4	0.052	0.082	0.63	_***	_****
H5	0.026	0.21	0.12	12	irregular
H6	0.021	0.041	0.51	_***	_****
H7	0.013	0.021	0.62	_***	_****
H8	0.010	0.082	0.12	21	irregular
H9	0.010	0.041	0.24	_***	_****
H10	0.0052	0.041	0.13	47	ellipsoid
H11	0.0026	0.021	0.13	58	sphere
H12	0.0010	0.041	0.25	44	_****
H13	0.0010	0.0082	0.13	140	sphere

\* Calculated from concentration of  $C_{16}$ TMABr and TMOS

\*\* Time precipitates appear after the addition of TMOS

\*\*\* Precipitation time could not be measured because of subtle change of solution.

\*\*\*\* Precipitation could not be recovered from the solution.

are shown in **Table 2**, and the TEM photographs of the particles are shown in **Fig. 2**. Although the shapes of particles were ellipsoidal in higher concentration (D1, D2), spherical particles were obtained in the wide range of the concentration of the reactants. Spheres were uniform when the concentration of TMOS was 0.028 mol/l and that of

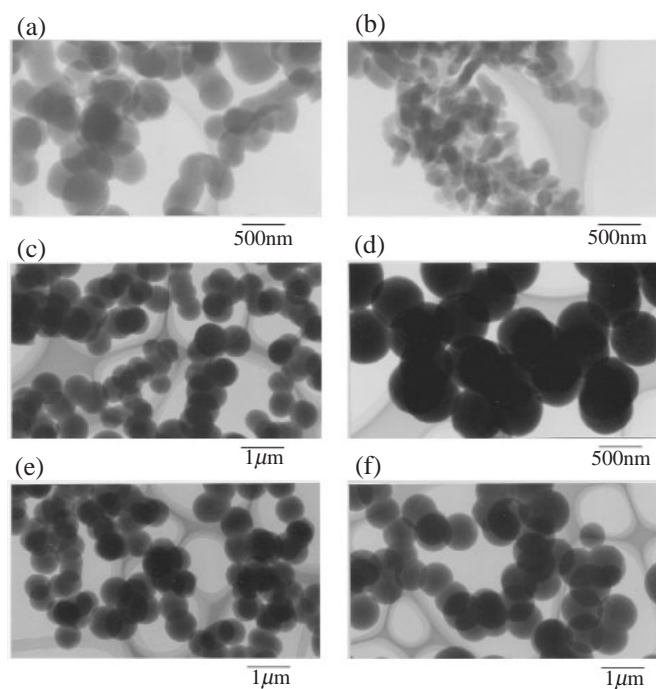


**Fig. 2** Transmission electron micrographs of (a) D1, (b) D2, (c) D3, (d) D6, (e) D7, and (f) D8.<sup>21)</sup>

$C_{12}TMABr$  was between 0.014 mol/l and 0.024 mol/l in particular. The X-ray diffraction patterns of these samples are given in **Fig. 3**, indicating the highly ordered hexagonal regularity (sample D6). Similar patterns were obtained for D1-D5 samples (XRD patterns not shown). With decreasing concentrations of the surfactant and silica, the peak of the (100) plane diffraction shifted to a lower 2-theta value (sample D7 and D8), and the peaks of the (100) and (210) planes became ambiguous. This fact indicates an enlargement of the mesopores and a disordering of the hexagonal regularity. The argon adsorption isotherm of sample D6 is shown in **Fig. 4**. The pore diameter calculated from the

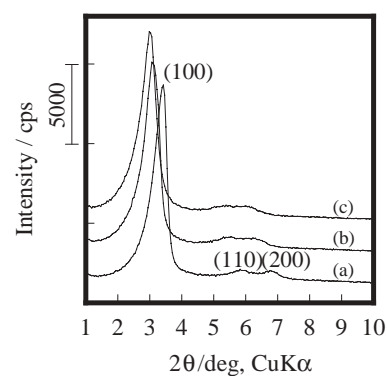


**Fig. 3** X-ray diffraction patterns of (a) D6, (b) D7, and (c) D8. X-ray diffraction patterns of D1, D2, and D3 were almost identical to that of D6.<sup>21)</sup>

**Table 2** Shapes of particles obtained from  $C_{12}TMABr$  and TMOS.<sup>21)</sup>

No.	Concentration of $C_{12}TMABr$ [mol/l]	Concentration of TMOS [mol/l]	$C_{12}TMABr/TMOS^*$	Precipitation time** [sec]	Shapes of particle
D1	0.052	0.41	0.13	6	ellipsoid and sphere
D2	0.052	0.082	0.63	9	ellipsoid
D3	0.026	0.21	0.12	19	sphere, partly adhered
D4	0.024	0.028	0.84	56	monodispersed sphere
D5	0.019	0.028	0.67	58	monodispersed sphere
D6	0.014	0.028	0.50	56	monodispersed sphere
D7	0.0094	0.016	0.59	107	sphere
D8	0.0047	0.012	0.39	158	sphere

\* Calculated from concentration of  $C_{12}TMABr$  and TMOS

\*\* Time precipitates appear after the addition of TMOS

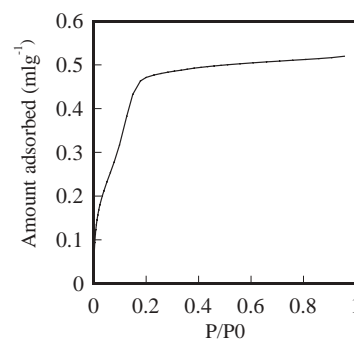


**Fig. 4** Argon adsorption isotherm of D6.<sup>21)</sup>

isotherm is 21.1 Å.

The  $C_{12}$ TMABr/TMOS ratios for the mono-dispersed spherical particle formation were from 0.5 to 0.84, which means that the syntheses proceeded under a condition where larger amount of surfactant was present than the amount of the surfactant (up to 0.15) that was actually taken into the pores. Thus, it is inferred that the presence of excessive surfactant leads to the uniformity in the spherical particles. On the basis of this inference, the concentrations of  $C_{10}$ TMABr and TMOS were also varied. The summarized results for the shapes and the uniformities of the particles are shown in **Table 3**, and the SEM photographs of the particles are shown in **Fig. 5**. When the TMOS and  $C_{10}$ TMABr concentrations were high, not only spherical particles, but also amorphous or sheet-shaped particles were precipitated (De1-De2). Only spherical particles were generated when the TMOS concentration was equal to or less than 0.082 mol/l, and the  $C_{10}$ TMABr concentration was equal to or less than 0.052 mol/l (De3-De6). Further, particles having a highly uniform particle size distribution with an average of 0.6  $\mu\text{m}$  were obtained when the TMOS concentration was 0.021 mol/l, and the concentration of  $C_{10}$ TMABr was 0.013 mol/l (De5). Moreover, under lower concentration conditions, mono-dispersed particles were obtained (De6). As the TMOS and  $C_{10}$ TMABr concentrations decreased, the precipitation time (i.e., the time from when TMOS was added until the particles started to precipitate) became longer. Thus, it is presumed that since the reaction proceeds slowly, particles with a uniform particle size are more likely to be generated. The X-ray diffraction patterns are shown in **Fig. 6**. Peak intensity of  $d_{100}$  was the highest when the TMOS concentration was 0.041 mol/l and

$C_{10}$ TMABr concentration was 0.026 mol/l (De4). These results indicated that the pores of this silica were at their most highly ordered. Under the conditions where the mono-dispersed particles were

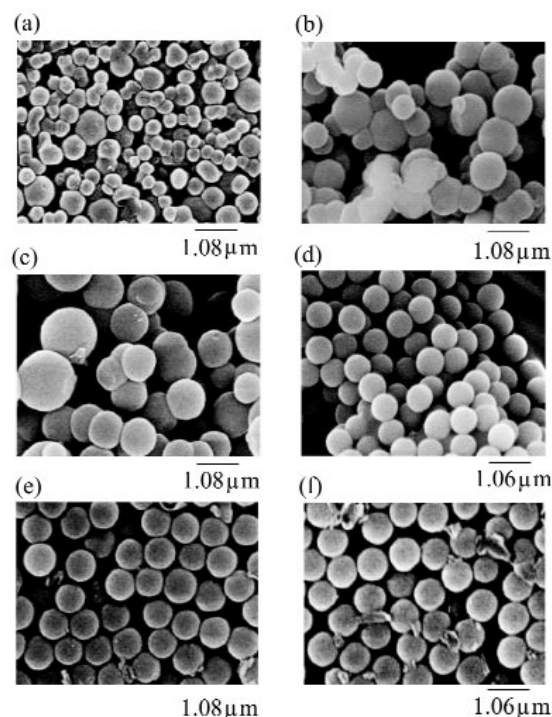


**Fig. 5** Scanning electron micrographs of (a) De2, (b) De3, (c) De4, (d) De5, (e) De8, and (f) De9.<sup>22)</sup>

**Table 3** Shapes of particles obtained from  $C_{10}$ TMABr and TMOS.<sup>22)</sup>

No.	Concentration of $C_{10}$ TMABr [mol/l]	Concentration of TMOS [mol/l]	$C_{10}$ TMABr/TMOS ratio	Precipitation time* [sec]	Shapes of particle	Average diameter [ $\mu\text{m}$ ]
De1	0.26	0.41	0.63	-	irregular	-
De2	0.086	0.14	0.63	-	irregular and sphere	-
De3	0.052	0.082	0.63	32	sheet and sphere	-
De4	0.026	0.041	0.63	-	sphere	0.84
De5	0.013	0.021	0.62	100	mono-dispersed sphere	0.60
De6	0.013	0.0051	2.5	570	mono-dispersed sphere	0.56
De7	0.01	0.021	0.48	120	mono-dispersed sphere	0.73
De8	0.0064	0.021	0.30	210	mono-dispersed sphere	0.67
De9	0.0064	0.010	0.64	420	mono-dispersed sphere	0.66

\* Time precipitates appear after the addition of TMOS



obtained (De5, De6), the  $d_{100}$  peak intensity was slightly lower and the half width was larger. These results indicated that the pores became less ordered.

### 3.2 Particle size control of mono-dispersed mesoporous silica spheres

Mono-dispersed spherical mesoporous silica was successfully synthesized from TMOS and surfactant with short alkyl-chain length ( $C_{12}$ TMABr and  $C_{10}$ TMABr). The concentration range where mono-dispersed spheres were obtained was wider when  $C_{10}$ TMABr was used as a surfactant. Next, synthesis was conducted using  $C_{10}$ TMABr as a surfactant in order to control the size of mono-dispersed spherical mesoporous silica. The synthesis temperature was varied under the concentration condition of De5 (TMOS: 0.021 mol/l, and  $C_{10}$ TMABr: 0.013 mol/l). The SEM photographs are shown in **Fig. 7**. Under this concentration condition, spherical particles were always generated regardless of the synthesis temperature, and mono-dispersed particles were obtained at a temperature of 50 °C or lower. Because the temperature of 60 °C is close to the boiling point of co-solvent methanol, the formation of mono-dispersed particles may be disturbed at this temperature. The higher the synthesis temperature,

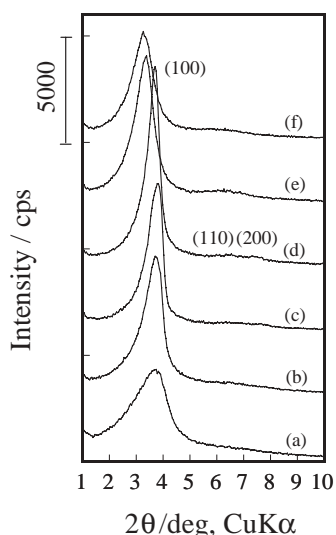


**Fig. 6** XRD patterns of calcined samples synthesized at different concentration. (a) De1, (b) De2, (c) De3 (d) De4, (e) De5, and (f) De9.<sup>22)</sup>

the smaller the average particle size; the size changed in the range from 0.6 to 0.96  $\mu\text{m}$ . When the synthesis temperature is lower, nucleation becomes less frequent, and the generation of large particles is more likely.

Subsequently, the methanol/water ratio was varied. The SEM photographs are shown in **Fig. 8**. Mono-dispersed spherical particles were obtained when the methanol/water ratio was equal to or less than 0.35, and the uniformity became particularly high when the ratio was within the range from 0.2 to 0.3. The average particle size became smaller, as the methanol/water ratio became smaller, in other words, as the relative amount of water increased. When the relative amount of water is large, it is expected that the large number of nuclei is generated. This leads to the formation of smaller

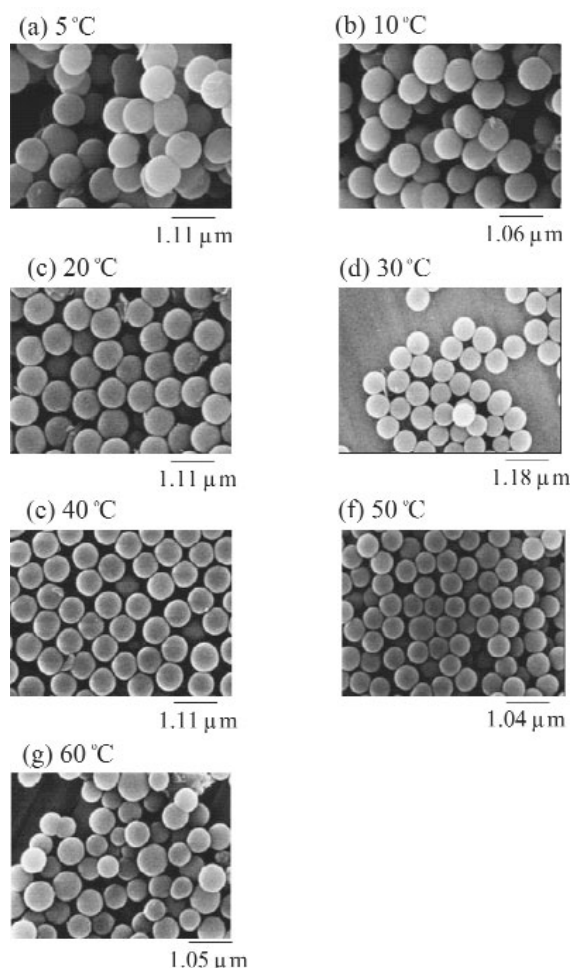


**Fig. 7** Scanning electron micrographs of calcined samples synthesized at different temperature. (a) 5 °C, (b) 10 °C, (c) 20 °C, (d) 25 °C, (e) 30 °C, (f) 40 °C, (g) 50 °C, and (h) 60 °C.<sup>22)</sup>

particles. The average particle size was controllable within the range from 0.5 to 0.74  $\mu\text{m}$  by varying the methanol/water ratio.

Then, alkoxysilanes with a different length of alkyl chains from TMOS were used as the Si source. The SEM photographs are shown in **Fig. 9**. Note that because TBOS was not dissolved at all in the methanol/water system, so only silica gel was generated. When TEOS was used, mono-dispersed particles with a particle size of approximately 1.2  $\mu\text{m}$  were obtained. This is more than double the size obtained from TMOS. This larger size is probably because TEOS has a lower reactivity than TMOS, and, therefore, the reaction proceeds more slowly. When TPOS was used, it was not completely dissolved in the methanol/water solvent, sheet-shaped particles as well as spherical particles were

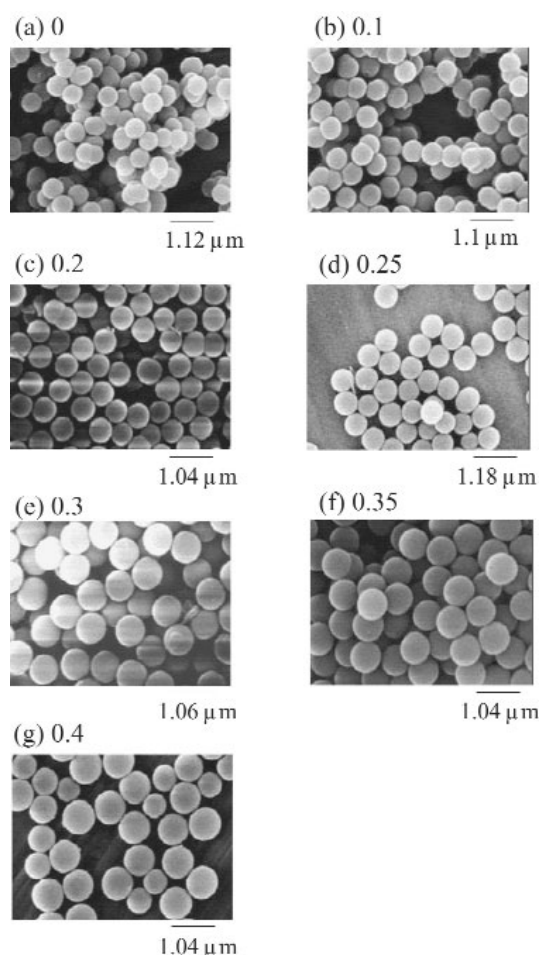


**Fig. 8** Scanning electron micrographs of calcined samples synthesized at different methanol/water ratio ( $r$ ). (a) 0, (b) 0.1, (c) 0.2, (d) 0.25, (e) 0.3, (f) 0.35, and (g) 0.4.<sup>22)</sup>

obtained.

In order to address the internal structure of the mono-dispersed spherical mesoporous silica, the partial incorporation of platinum was used.<sup>23)</sup> The amount of platinum incorporated was further controlled and well optimized for the clear observation of inside of the sphere. A TEM image of platinum incorporated De5 is given in **Fig. 10**. Dark section of the micrograph represents the

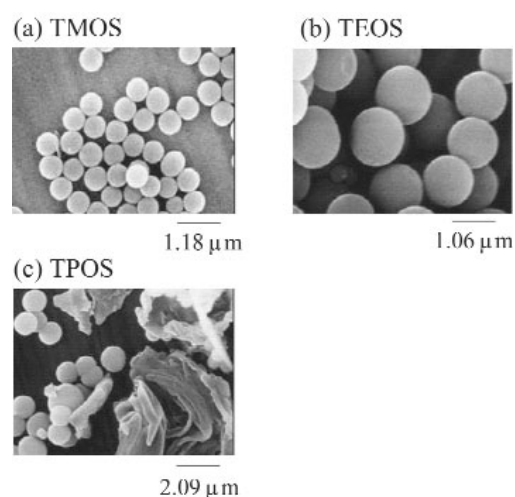


**Fig. 9** Scanning electron micrographs of calcined samples synthesized with different tetra alkoxysilane (a) TMOS, (b) TEOS, and (c) TPOS.<sup>22)</sup>

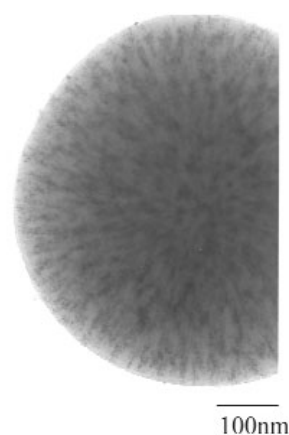


**Fig. 10** Transmission electron micrograph of platinum incorporated De5. Dark section represents the platinum.<sup>22)</sup>

platinum incorporated into the pores. As shown in Fig. 10, pores are uniformly aligned radially from the center toward the periphery of the spherical particle. In general, it is impossible to constitute such an alignment with a highly ordered hexagonal structure. As apparent from Fig. 6, the particles obtained in this study had a less ordered hexagonal structure. This structure enabled a radial structure of the mesopores like this. It is inferred that mesopores grow from center to outside the sphere radially.

#### 4. Conclusions

Mono-dispersed spherical mesoporous silica with highly ordered hexagonal regularity was successfully synthesized by reacting TMOS and C<sub>12</sub>TMAB under very specific concentrations. Further, when C<sub>10</sub>TMAB was used as a surfactant, the particle size of the mono-dispersed spherical mesoporous silica was changed by varying synthesis temperature, water/methanol ratio, and silica source while the mono-dispersion characteristics were retained. The pores were aligned from the center toward the periphery of the spherical particles. The obtained mono-dispersed spherical mesoporous silica had a particle size equivalent to the wave lengths of visible light, and thus its application to an optical use such as photonic crystal is expected.

#### References

- 1) Kresge, C. T., Leonowicz, M. E., Roth, W. J., Vartuli, J. C. and Beck, J. S. : *Nature*, **359**(1992), 710
- 2) Beck, J. S., Vartuli, J. C., Roth, W. J., Leonowicz, M. E., Kresge, C. T., Schmitt, K. D., Chu, C. T.-W., Olson, D. H., Sheppard, E. W., McCullen, S. B., Higgins, J. B. and Schlenker, J. L. : *J. Am. Chem. Soc.*, **114**(1992), 10834
- 3) Yang, P., Zhao, D., Chmelka, B. F. and Stucky, G. D. : *Chem. Mater.*, **10**(1998), 2033
- 4) Bruinsma, P. J., Kim, A. Y., Liu, J. and Baskaran, S. : *Chem. Mater.*, **9**(1997), 2507
- 5) Lin, H.-P., Yang, L.-Y., Mou, C.-Y., Lee, H.-K. and Liu, S.-B. : *Stud. Surf. Sci. Catal.*, **129**(2000), 7
- 6) Tolbert, S. H., Schaffer, T. E., Feng, J., Hansma, P. K. and Stucky, G. D. : *Chem. Mater.*, **9**(1997), 1962
- 7) Kim, J. M., Kim, S. K. and Ryoo, R. : *Chem. Commun.*, (1998), 259
- 8) Guan, S., Inagaki, S., Ohsuna, T. and Terasaki, O. : *J. Am. Chem. Soc.*, **122**(2000), 5660
- 9) Shunai, C., Sakamoto, Y., Terasaki, O. and Tatsumi, T. : *Chem. Mater.*, **13**(2001), 2237
- 10) Qi, L., Ma, J., Cheng, H. and Zhao, Z. : *Chem. Mater.*, **10**(1998), 1623
- 11) Lin, H.-P., Cheng, Y.-R. and Mou, C.-Y. : *Chem. Mater.*, **10**(1998), 3772
- 12) Huo, Q., Feng, J., Schuth, F. and Stucky, G. D. : *Chem. Mater.*, **9**(1997), 14
- 13) Stöber, W., Fink, A. : *J. Colloid and Interface Sci.*, **26**(1968), 62
- 14) Grün, M., Büchel, G., Kumar, D., Schumacher, K., Bidlingmayer, B. and Unger, K. K. : *Stud. Surf. Sci. Catal.*, **128**(2000), 155
- 15) Grün, M., Lauer, I. and Unger, K. K. : *Adv. Mater.*, **9**(1997), 254
- 16) Schumacher, K., Renker, S., Unger, K. K., Ulrich, R., Chesne, A. D., Spiess, H. W. and Wiesner, U. : *Stud. Surf. Sci. Catal.*, **129**(2000), 1
- 17) Luo, Q., Li, L., Xue, Z. and Zhao, D. : *Stud. Surf. Sci. Catal.*, **129**(2000), 37
- 18) Inagaki, S., Koiwai, A., Suzuki, N., Fukushima, Y. and Kuroda, K. : *Bull. Chem. Soc. Jpn.*, **69**(1996), 1449
- 19) Anderson, M. T., Martin, J. E., Odinek, J. G. and Newcomer, P. P. : *Chem. Mater.*, **10**(1998), 311
- 20) Anderson, M. T., Martin, J. E., Odinek, J. G. and Newcomer, P. P. : *Chem. Mater.*, **10**(1998), 1490
- 21) Yano, K., Suzuki, N., Akimoto, Y. and Fukushima, Y. : *Bull. Chem. Soc. Jpn.*, **75**(2002), 1977
- 22) Yano, K. and Fukushima, Y. : *J. Mater. Chem.*, **13**(2003), 2577
- 23) Ko, C. H. and Ryoo, R. : *Chem. Commun.*, (1996), 2467

(Report received on Dec. 12, 2004)



**Kazuhisa Yano**

Research fields : Porous material

Academic degree : Dr. Eng.

Academic society : Chem. Soc. Jpn., Soc. Polym. Sci. Jpn.